Zehui *et al.*
Journal of Engineering and Applied Science (2024) 71:162
https://doi.org/10.1186/s44147-024-00492-w

Journal of Engineering and Applied Science

RESEARCH Open Access

Study on bending fatigue performance of recycled aggregate backfill subgrade

Chen Zehui[1*], Feng Xiaowei[2], Fang Xinjun[3] and Wu Shijun[1]

*Correspondence:
18868571036@163.com

[1] Zhejiang Guangsha Vocational and Technical University of Construction, Dongyang City, Zhejiang Province 322100, China
[2] Zhejiang Scientific Research Institute of Transport, Hangzhou City, Zhejiang Province 310023, China
[3] Zhejiang Hangkun Construction Group Co., Ltd, Hangzhou City, Zhejiang Province 310015, China

Abstract

Recycled aggregate (RA), as a backfill subgrade material, has strong reproducibility and environmental protection, which cannot only effectively reduce resource consumption and environmental pollution but also achieve recycling of resources. Therefore, a study on the bending fatigue performance of RA backfill subgrade is proposed. Based on linear elastic state, softening state, and damage accumulation state, the variation law of bending fatigue damage variables is analyzed, and the stiffness of RA under cyclic load is calculated. According to the correlation between fatigue damage corresponding to two different load links and the constitutive relationship of RA, the identification results of bending fatigue damage state based on RA backfilling subgrade is obtained. The advantages of the fatigue damage model of RA are analyzed, and the fatigue life equation is established based on the damage evolution equation. Strain, stiffness modulus, asphalt saturation, and asphalt mixture adjustment coefficient are selected as model parameters to establish the fatigue damage model of RA. The flexural bearing capacity of the double-reinforced rectangular section is calculated, and the flexural fatigue performance of RA backfill subgrade is analyzed. The test results show that the high stress level in this method leads to a sharp decline in the fatigue life of the specimen, and the influence of fatigue damage gradually appears, which is helpful to improve the durability and safety of the subgrade structure. The range of change shows a small range, which is close to the reduction coefficient result, indicating that this method has high reliability in analyzing the bending fatigue performance of RA backfill subgrade.

Keywords: Recycled aggregate (RA), Backfill subgrade, Bending fatigue, Performance research, Fatigue damage, Fatigue life equation

Introduction

Backfilling subgrade with RA is a road engineering technology with environmental protection and resource-saving benefits. It utilizes RA as filling material to construct the subgrade. RA, as a backfill subgrade material, exhibits strong reproducibility and environmental protection. It not only effectively reduces resource consumption and environmental pollution but also facilitates resource recycling, thus offering broad application prospects [1, 2]. However, due to the differences between RA and traditional subgrade materials, its characteristics and properties may also lead to some special problems in subgrade usage, the most significant of which is bending

fatigue [3]. Bending fatigue performance is one of the key indicators for evaluating the suitability of subgrade materials under traffic loads [4]. RA backfill subgrade is subjected to repeated vehicle loadings in practical use and experiences long-term deformation due to traffic loads, making its crack resistance and fatigue performance crucial factors directly impacting the reliability and safety of the entire subgrade [5]. Comprehensive insights into the durability of RA backfill subgrade materials under different conditions can be gained through in-depth studies on their bending fatigue performance. This provides a scientific basis for engineering design and construction, ensuring the long-term stability and safe operation of roads [6, 7]. Therefore, studying the bending fatigue performance of RA backfill subgrade materials is of paramount significance for enhancing the durability, safety, and sustainability of road engineering. In reference [8], a reproduction with limited components for reusing, collective, self-compressed, concrete-filled short tubular steel columns is presented, using the ABAQUS simulation software to analyze the mechanical features of nine different groups of such columns subjected to axial compression. By juxtaposing the outcomes of the limited components reproduction with experimental findings, it is observed that the load-vertical strain curve simulated aligns well with experimental results. Moreover, the full discrepancy in the final bearing capacity between reproduction and experimental measurements does not exceed 3%. Notably, the final bearing capacity of the examples exhibits a declining trend as the proportion of RA content increases. Reference [9] proposes to investigate the impact of recycled concrete aggregate on the hardening performance of self-compacting concrete. With the continued development of countries worldwide, a significant quantity of recycled concrete aggregates has been generated from numerous construction and demolition projects, with their production steadily increasing over the past few decades. A practical approach to managing recycled concrete aggregate waste involves reusing them as aggregates in concrete production. In modified self-compacting concrete, 5 ~ 10 mm crushed recycled concrete aggregates with varying proportions are utilized to assess their viability as substitutes for natural aggregates. Reference [10] introduces the concept of proportional concrete beams featuring the highest content of coarse RA: a structural verification for precast concrete building applications. The utilization of RAs enhances the sustainability of concrete. This study reports an experimental initiative involving precast concrete manufacturers. Bending, shear bending, shear, and long-term deflection tests were conducted on scaled beams. The mixture demonstrates low bearing capacity post-failure, with limited compliance with the deflection limit set by the long-term deflection test. Reference [11] enhances the bond performance of embedded ribbed steel bars in RA concrete through the utilization of steel mesh fabric constraints. To investigate the bond performance of passively confined RA concrete, central pull-out tests on deformed steel bars with a diameter of 12 mm were conducted. The replacement rate of recycled concrete aggregate ranges from 0 to 100%. Considering the influence of concrete grade, RA concrete content, steel mesh fabric constraints, and transverse lacing, a new formula for calculating the ultimate bond strength of RA concrete is proposed, yielding results consistent with experimental findings.

Based on the aforementioned research, this paper conducts an in-depth study on the bending fatigue performance of RA backfill subgrade materials. This study provides

Table 1 Concrete mix proportion /(kg/m^3)

Concrete type	RAC-0	RAC-50	RAC-100
Cement	343	343	343
Flyash	148	148	148
Crushi	762	762	762
Natural coarse aggregate	1003	501	0
Recycled coarse aggregate	0	468	935
Water	206	206	206

Table 2 Structure parameter table of recycled aggregate

Parameter	Base (subbase)	Surface layer (surface layer)
Location	The lower level in the recycled aggregate structure layer	The upper layer in the recycled aggregate structure layer
Function	It bears the functions of transferring load, dispersing load, and providing support	Responsible for bearing vehicle load, providing comfortable driving conditions, and preventing waterlogging
Main function	Share the traffic load, improve the overall bearing capacity, and reduce the settlement and deformation	Smooth surface, higher requirements for driving comfort, enhancing the stability and durability of subgrade structure

support for promoting the application of RA in road engineering and advancing the development of road engineering technology.

Materials

P·O42.5 ordinary Portland cement is used as the cement. Sand comprises natural river sand. The fineness of fly ash is 21%. Natural coarse aggregate consists of continuously graded crushed stone, while recycled coarse aggregate is obtained by crushing concrete specimens demolished in the concrete laboratory, with a water absorption rate of 5.3%. Both aggregates are continuously graded with a particle size ranging from 5.0 to approximately 20.0 mm.

The concrete mix is presented in Table 1. RAC-0 represents natural aggregate concrete, RAC-50 denotes recycled coarse aggregate concrete with a replacement rate of 50%, and RAC-100 signifies recycled coarse aggregate concrete with a replacement rate of 100%.

For concrete with three mix proportions, three cubic specimens with the size of 150 mm × 150 mm × 150 mm and seven trabecular specimens with the size of 100 mm × 100 mm × 500 mm are poured in each batch.

Table 2 displays the structural combination of RA and the corresponding calculation parameters. Assuming that the parameters of RA are not affected by temperature, RA is typically divided into two structural layers: the base layer and the surface layer in subgrade engineering. The details are as follows:

(1) Base (subbase): The base is the lower level in the RA structure layer, which undertakes the functions of load transfer, load dispersion, and support provision. It is typically situated directly on the subgrade soil and is constructed by backfilling RA or RA

concrete. The primary function of the base is to distribute the traffic load, enhance the overall bearing capacity, and minimize settlement and deformation.

(2) Pavement (surface layer): The pavement serves as the upper layer in the RA structure layer, constituting the section of the road traversed directly by vehicles. Its primary functions include bearing the vehicle load, offering comfortable driving conditions, and preventing waterlogging. Typically, the surface layer is laid with RA mixture or RA asphalt concrete, featuring a smooth surface and necessitating high driving comfort.

Auxiliary structural layers, such as isolation layers or filter layers, can be installed between the base course and the surface course according to specific engineering requirements to enhance the stability and durability of the subgrade structure. By carefully designing and selecting the combination mode of RA structure layers, the benefits of RA can be fully utilized, thereby achieving the objectives of energy conservation, environmental protection, and resource recycling in subgrade engineering.

Six standard RA specimens were prepared in this experiment, namely A-1#, B-1#, C-1#, D-1#, E-1#, and F-1#. The A-1# specimen was selected, with a section size of 100 mm × 160 mm, featuring main reinforcement of 2 ϕ 10 at the bottom of the beam and stirrups of 2 ϕ 6. The specific structure is illustrated in Fig. 1.

Instrument

The AST asphalt mixture standard tester is utilized in the test. AST asphalt mixture standard tester is a new concept product introduced by IPC and is a multifunctional test equipment. AST features a large-size, double-door temperature control box. The specimen is placed within the temperature control box, and a certain frequency load is applied to the top of the specimen. The force and displacement of the specimen are

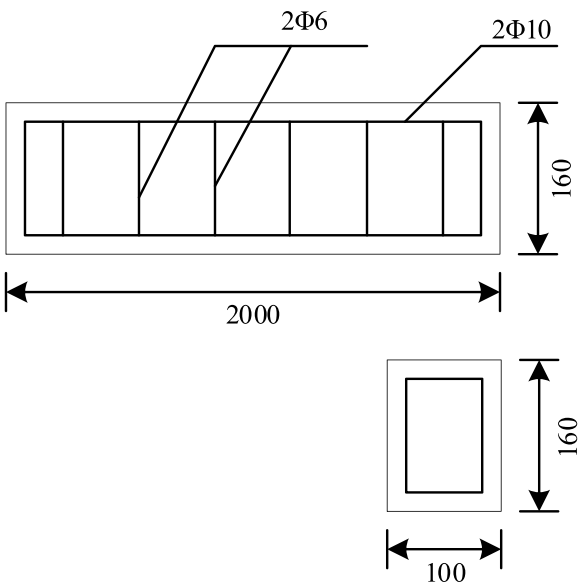

Fig. 1 Specimen size and reinforcement diagram

Fig. 2 Structure diagram of AST asphalt mixture standard tester

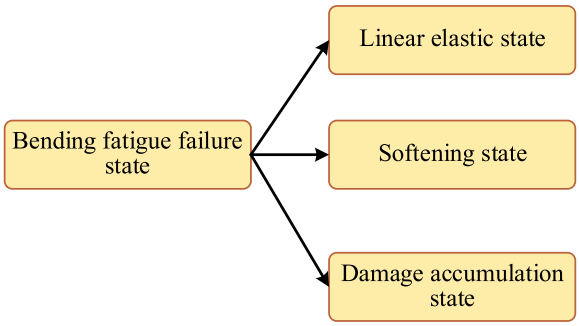

Fig. 3 Structural diagram of bending fatigue failure state

recorded by the sensor, enabling the calculation of the dynamic modulus of the specimen. The equipment is depicted in Fig. 2.

Methods

Recognition of bending fatigue failure state of recycled aggregate backfill subgrade

RA is extensively utilized in subgrade engineering, effectively harnessing waste resources and mitigating the demand for natural stone. However, owing to the disparity in properties between RA and natural aggregate, their performance and behavior in subgrade differ [12]. To identify the failure state, strain sensors are installed on the subgrade to monitor its strain distribution in real-time [13].

Based on the aforementioned test materials and instruments, there are typically three distinct fatigue damage processes corresponding to the actual load of RA when identifying the bending fatigue failure state based on RA backfilling subgrade [14]. These three states include the linear elastic state, softening state, and damage accumulation state. The detailed structural diagram is depicted in Fig. 3.

(1) Linear elastic state: During the cyclic loading and unloading process, RA exhibits linear elastic behavior, with its stress and strain linearly changing in response to loading and unloading [15]. In this state, RA shows no obvious signs

of fatigue failure, and its characteristics under unloading conditions are similar to those under loading conditions [16].

(2) Softening state: After repeated cyclic loading, RA begins to exhibit a certain degree of softening. At this stage, the stress–strain response curve of the material deviates from the linear elastic state, leading to stress softening. The softening state arises from the accumulation of damage to the internal structure of the material during cyclic loading, which can be identified by changes in the tangent elastic modulus (tangent slope) [17].

(3) Damage accumulation state: When RA is subjected to higher stress or strain during cyclic loading, damage gradually accumulates within the material. In this state of damage accumulation, the strength and stiffness of RA progressively decrease, and noticeable signs of fatigue failure emerge, such as the generation and propagation of cracks [18]. At this stage, the failure characteristics of materials must account for the behavior under unloading conditions to accurately depict the fatigue damage process of RA.

Under the condition of cyclic loading, the cumulative damage during the cyclic loading/unloading process is defined. The variation law of bending fatigue damage variables is described according to each loading/unloading cycle, as shown in Formula (1):

$$\begin{cases} A = a \times \left(\frac{maxH}{c} - b\right) \times D_F, D_F \geq 0 \\ A' = 0, D_F < 0 \end{cases} \tag{1}$$

In Formula (1), a, b, and c all represent the damage accumulation speed of RA, and $maxH$ represents the upper limit of effective stress experienced by RA; D_F stands for fatigue damage variable. According to Formula (1), A gradually increases in the loading link, $A\prime$ is set to 0 again in the unloading link, and the fatigue damage variable is less than 0, thus ensuring the continuous increase of the cumulative speed of $A\prime$.

The fluctuation of RA characteristics can be described by A and $A\prime$, that is, the constitutive relation of RA can be described. Use Formula (2) to describe the stiffness of RA under cyclic load, and the formula is:

$$\begin{cases} \frac{d\alpha_a}{d\beta_b} = A \times \left(\frac{max\alpha_a}{max\beta_b}\right) \\ \frac{d\alpha_c}{d\beta_d} = A\prime \times \left(\frac{max\alpha_c}{max\beta_d}\right) \end{cases} \tag{2}$$

In Formula (2), $\frac{d\alpha_a}{d\beta_b}$ represents the normal tangent stiffness under the current load condition; $max\alpha_a$ and $max\beta_b$ respectively represent the normal stress value and displacement value at the end of the previous load; $\frac{d\alpha_c}{d\beta_d}$ represents tangential stiffness under the current load condition; $max\alpha_c$ and $max\beta_d$ respectively represent the tangential stress value and displacement value at the end of the previous load.

Formula (3) can be used to describe how the stress and strain of RA decrease from the upper limit to the origin under the condition of cyclic load unloading, indicating the accumulation of damage within the unloading process. The formula is as follows:

$$\begin{cases} \frac{\alpha_a}{\beta_b} = \left(\frac{max\alpha_a}{max\beta_b}\right) \times \frac{d\alpha_a}{d\beta_b} \\ \frac{\alpha_c}{\beta_d} = \left(\frac{max\alpha_c}{max\beta_d}\right) \times \frac{d\alpha_c}{d\beta_d} \end{cases} \tag{3}$$

The above process elucidates the correlation between the fatigue damage corresponding to two different loading links and the constitutive relation of RA under cyclic load [19]. From this, the identification results of the bending fatigue failure state based on RA backfilling subgrade can be derived, as expressed by the following formula:

$$max\chi = \alpha_a \times \beta_b \times \alpha_c \times \beta_d \tag{4}$$

Formula (4) shows that the identification result of bending fatigue failure state of RA can be defined, and according to this result, data can be provided for building the fatigue damage model of RA.

Construction of fatigue damage model of recycled aggregate

The fatigue damage model of RA is a mathematical model employed to describe the development of damage and the failure process of RA under fatigue loading. This model is based on experimental data and theoretical analysis of RA under bending fatigue loading, establishing a mathematical framework to depict the fatigue life and the evolution of damage in RA [20]. The damage process of RA under fatigue loading can be expressed through mathematical equations and parameters, as illustrated in Fig. 4, which showcases its advantages.

(1) Nonlinear: The fatigue damage model of RA typically exhibits nonlinear characteristics because the process of damage accumulation in RA under fatigue loading is often nonlinear, and the rate of damage may vary with the increase in load cycles [21].
(2) Multi-parameters: To accurately describe the fatigue damage features of RA, the model typically incorporates multiple parameters, including the strength, ultimate stress, and crack growth rate of the material [22].
(3) Historical dependence: Recognizing that the damage of RA under fatigue loading is a historically dependent process, meaning that the previous load history influences the current damage state, the model may need to account for historical bearing capacity [23].

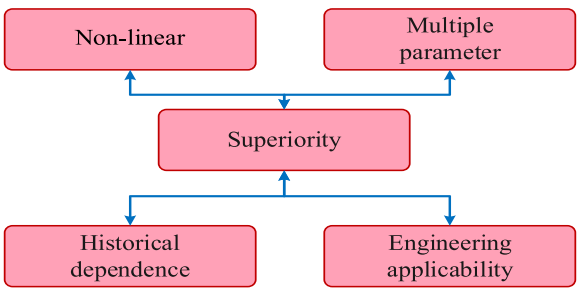

Fig. 4 Superiority structure diagram of fatigue damage model of recycled aggregate

(4) Engineering applicability: The fatigue damage model of RA is intended for application in actual subgrade engineering, thus requiring reliability, accuracy, and conciseness.

Creep and fatigue damage will occur when RA is used to backfill subgrade under repeated load [24], which will shorten the life of RA. The creep damage V of RA is as follows:

$$V = \frac{T_1 \times N_2 \times G_3 \times M_4}{max\chi} \tag{5}$$

In the formula, T_1 stands for time; N_2 represents the fatigue damage of RA; G_3 stands for temperature; M_4 stands for load stress. The fatigue damage of RA can be described by the following formula:

$$J = V \times N_{FG} \times \overline{\sigma} \times \sigma_M \tag{6}$$

In the formula, N_{FG} represents the number of loads; $\overline{\sigma}$ stands for average stress; σ_M stands for bending and tensile stress.

Considering the coupling between fatigue damage and creep damage, the following damage evolution equation is defined, and the formula is:

$$dD = \frac{dD_a + dD_b + dD_c}{J} \tag{7}$$

In the formula, dD_a represents creep-fatigue damage of RA; dD_b stands for tensile stress; dD_c represents the gradation coefficient of the mixture.

Based on the damage evolution equation, the fatigue life equation is established, and the formula is:

$$F_{RT} = \frac{dD}{R_P \times R_Q \times R_W} \tag{8}$$

In the formula, R_P represents the initial tensile strain; R_Q represents the initial stiffness modulus; R_W stands for asphalt saturation. Based on the fatigue life equation, strain, stiffness modulus, asphalt saturation, and adjustment coefficient of asphalt mixture are selected as model parameters, and the fatigue damage model of RA is established. The formula is:

$$N_F = \frac{K_1 \times \mu + K_2 \times \kappa + K_3 \times \theta + K_4 \times \zeta}{F_{RT}} \tag{9}$$

In the formula, K_1, K_2, K_3, and K_4 all represent regression coefficients; μ stands for strain; κ represents stiffness modulus; θ represents asphalt saturation; ζ represents the adjustment coefficient of asphalt mixture.

Analysis of bending fatigue performance of recycled aggregate backfilled subgrade

RA backfill subgrade is subjected not only to static loads in practical application but also to cyclic actions of varying loads [25]. When subjected to loading, the section of the subgrade filled with RA will experience the combined effects of bending moments and

shear forces, potentially resulting in bending fatigue failure of the subgrade filled with RA under repeated exposure to both.

For the RA backfill subgrade, the ultimate reinforcement ratio is set as L_V, and when the set reinforcement ratio is less than L_V, it means that the RA backfill subgrade is in a state of bending fatigue failure. On the contrary, it indicates that the subgrade backfilled with RA is in a state of shear fatigue failure. Through repeated tests, it can be determined that the RA backfill subgrade is subjected to both bending moment and shear force. When the stress level of cyclic load is relatively high, with the continuous increase in load cycles, it may lead to shear fatigue failure of the RA backfill subgrade in random areas [26].

Fatigue load can also be referred to as disturbance stress, which primarily pertains to stress that varies over time. Among these variations, the load can be categorized into stress and displacement. Load spectrum mainly refers to the regular curve formed by the change of load over time, and the specific calculation formula is as follows:

$$\begin{cases} \triangle P = P_{\max} - P_{\min} \\ P_m = \frac{P_{\max} - P_{\min}}{2} \end{cases} \tag{10}$$

In the formula, $P_{\max}$ and $P_{\min}$ represent the maximum and minimum pressures, respectively. When analyzing the bending fatigue performance of RA backfill subgrade, various tests are typically conducted to acquire the corresponding fatigue performance test data. However, since actual data often contain a few outliers and exhibit noticeable dispersion, it is usually necessary to employ statistical analysis methods to process the test data during fatigue analysis. Processing test data through statistical analysis methods can aid in clearly understanding the fatigue performance of RA backfill subgrade materials and components. The internal and external factors contributing to bending fatigue can be better analyzed simultaneously through the statistical analysis of the data. In the process of analyzing the bending fatigue performance of reclaimed aggregate backfill subgrade, different tests are primarily used to obtain the corresponding fatigue performance test data. As there will inevitably be a small number of discrete points in actual data, showing significant dispersion, the test data are predominantly processed through statistical analysis during fatigue analysis. The fatigue performance of RA backfills subgrade materials and components, along with the internal and external factors influencing bending fatigue, can only be clearly comprehended by processing the data.

The calculation formula for the bending moment bearing capacity of a double-reinforced rectangular section is as follows:

$$B = B_1 \times B_2 \times B_3 \times B_4 \tag{11}$$

In the formula, B_1 represents the total compressive strength of RA; B_2 represents the cross-sectional area of RA under pressure; B_3 represents the maximum pressure on the normal section; B_4 represents the total length of RA.

In order to effectively prevent the deformation of RA, it is necessary to meet the following constraints ρ_2:

$$B \leq D_Z \tag{12}$$

In the formula, D_Z represents the diameter of RA.

During the surface reinforcement process of reclaimed aggregate backfill subgrade, the bending fatigue performance of the subgrade is calculated according to the following flowchart, as depicted in Fig. 5.

The specific steps are as follows:

Step 1: Solve the initial strain δ_0 of the edge under the action of the bending moment of the reclaimed aggregate backfill subgrade.

Step 2: Calculate the effective tensile strain ε_1 of reclaimed aggregate backfill subgrade by Formula (13) when it reaches the ultimate compressive strain.

$$\varepsilon_1 = \delta_0 \times S_i \times Q_i \times K_i \tag{13}$$

In the formula, S_i represents the compressive cross-sectional area of RA; Q_i represents the axial strength of reclaimed aggregate backfill subgrade; K_i represents the compressive strength value of steel bar.

Step 3: Determine the effective strain of reclaimed aggregate backfill subgrade.

Step 4: Calculate the reduction factor X_C of the equivalent stress model of the subgrade filled with compressed RA, as shown in Formula (14):

$$X_C = S_j \times \varepsilon_1 \tag{14}$$

In the formula, S_j represents the effective cross-sectional area of subgrade backfilled with RA.

Step 5: Calculate the interface bending moment of the reinforced RA backfill subgrade. Therefore, the bending fatigue performance of RA backfill subgrade is studied.

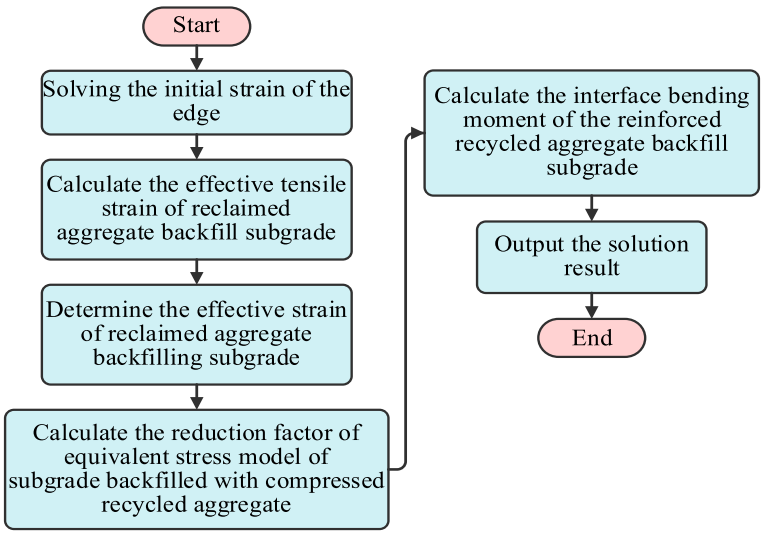

Fig. 5 Flow chart of bending fatigue performance analysis of reclaimed aggregate backfill subgrade

Results and discussion

In order to validate the research on the bending fatigue performance of RA backfill subgrade, experiments were conducted.

During the test, the fatigue damage model of RA was introduced to measure the cumulative fatigue damage of the specimen. The model relies on the degree of attenuation of the elastic modulus of the specimen to assess the development of fatigue damage in the specimen, and the expression is as follows:

$$L = 1 - \frac{\psi_1}{\psi_0} \tag{15}$$

In the formula, ψ_1 represents the elastic modulus of the specimen after fatigue damage; ψ_0 represents the initial elastic modulus of the specimen. According to Formula (15), the variation of fatigue cumulative damage with stress level of six standard RA specimens in this test can be counted, and the results are shown in Fig. 6:

As depicted in Fig. 6, the evolution process of fatigue cumulative damage of RA specimens is divided into three main stages: When the stress level is less than 0.3, the fatigue cumulative damage score of specimens exhibits a sharp upward trend. Even at lower stress levels, the fatigue damage of the specimen accumulates and intensifies rapidly, indicating that the specimen will suffer from more serious fatigue damage at lower stress levels. When the stress level is between 0.3 and 0.8, the cumulative fatigue damage score of the specimen remains relatively stable, with a slow growth rate. The specimen still experiences a certain degree of fatigue damage at medium stress levels, but the growth rate is slower than that observed in the previous stage. When the stress level exceeds 0.8, the fatigue cumulative damage score of the specimen increases significantly again, and the overall stiffness of the specimen begins to decrease, with fatigue loss becoming more pronounced. Through this method, it is evident that high stress levels lead to a sharp decline in the fatigue life of specimens, with the influence of fatigue damage gradually becoming apparent. This information is beneficial for evaluating the fatigue performance characteristics of RA in practical engineering applications, guiding the design

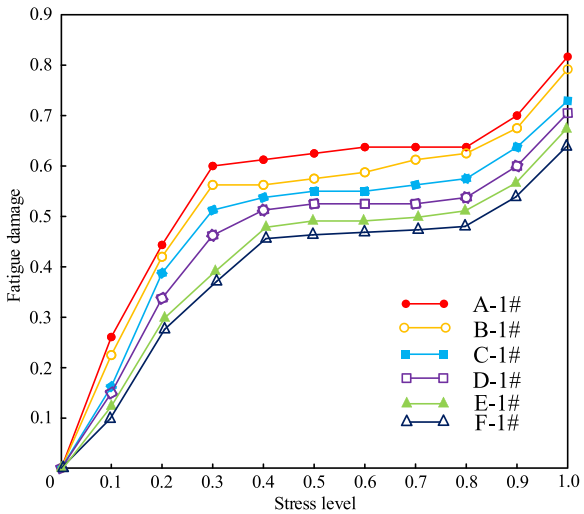

Fig. 6 Fatigue cumulative damage results of different recycled aggregate specimens

and selection of suitable RA materials, and further enhancing the durability and safety of subgrade structures.

In order to validate the overall efficiency of the approach suggested in this study, the techniques outlined in citations [8] and [9] have been chosen for comparative analysis. The fatigue damage of RA is measured using the aforementioned methods, and the range is utilized as the test index to compare the analysis accuracy of different methods. The test outcomes are presented in Table 3.

From Table 3, it is evident that the extreme values obtained using this method fluctuate less than those obtained using reference [8] and reference [9] under each load condition. In most cases, the extreme values obtained using this method are lower than those obtained using the other two methods, indicating that this method exhibits good stability and consistency in studying the bending fatigue performance of RA backfill subgrade. Based on the data comparison, it can be concluded that this method provides relatively more reliable and consistent results when evaluating the bending fatigue performance of RA backfill subgrade. The extreme range obtained using this method shows a minimal range of change, signifying high accuracy and precision in experimental design, data acquisition, or analysis.

The test results mentioned above are input into the fatigue damage model of RA as variable values for calculation. The reduction coefficient results of the equivalent stress model of compressed RA backfill subgrade are compared with the test results to determine accuracy. The reduction factor is a parameter used to account for the deviation between the actual fatigue life of materials and the theoretical prediction value. It is typically employed to correct fatigue test data to obtain more realistic and reliable results. The comparison test results are illustrated in Fig. 7.

As depicted in Fig. 7, the method proposed in this paper closely aligns with the reduction coefficient result, indicating its high reliability in analyzing the bending fatigue performance of RA backfill subgrade. Moreover, the accuracy of analyzing the bending fatigue performance of RA backfill subgrade is high, enabling a more precise evaluation of the actual fatigue life of materials. This further demonstrates that the method proposed in this paper comprehensively considers the actual working conditions, loading

Table 3 Comparison outcomes of range of different methods

Load times	Extreme difference/%		
	The method in this paper	Reference [8] method	Reference [9] method
1	0.02	0.25	0.17
2	0.03	0.21	0.26
3	0.01	0.34	0.38
4	0.02	0.32	0.47
5	0.02	0.40	0.55
6	0.03	0.44	0.64
7	0.01	0.56	0.77
8	0.01	0.55	0.88
9	0.01	0.64	0.91
10	0.02	0.67	0.99

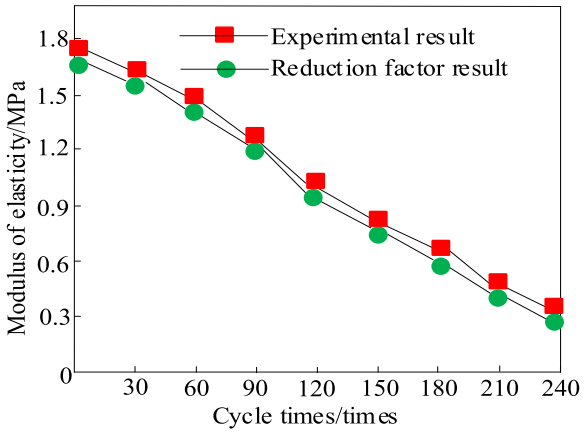

Fig. 7 Comparison results of reduction factor and test results

conditions, and the authenticity of test data in fatigue performance analysis, thereby better reflecting the fatigue performance of RA backfill subgrade in the actual usage environment.

Conclusions

Through the research on the bending fatigue performance of RA backfill subgrade, the following conclusions can be drawn:

The main results are as follows:

(1) The high stress level in this method leads to a sharp decline in the fatigue life of specimens, and the influence of fatigue damage gradually appears. This finding is helpful in evaluating the fatigue performance characteristics of RA in practical engineering applications, guiding the design and selection of suitable RA materials, and further improving the durability and safety of subgrade structures.

(2) The method proposed in this paper can provide relatively more reliable and consistent results when evaluating the bending fatigue performance of RA backfill subgrade. Additionally, the range shows a small range of change, indicating high accuracy and precision in experimental design, data collection, or analysis.

(3) The method proposed in this paper closely aligns with the result of the reduction coefficient, demonstrating its high reliability in analyzing the bending fatigue performance of RA backfilled subgrade. Furthermore, the accuracy in analyzing the bending fatigue performance of RA backfilled subgrade is high, enabling a more precise evaluation of the actual fatigue life of materials.

Further research in the future should focus on the following aspects:

(1) Strengthening the engineering technology research of reclaimed aggregate backfilling subgrade. In practical engineering, there are still some challenges in construction technology, test methods, and quality control of reclaimed aggregate backfill subgrade. Therefore, future research could concentrate on enhancing the engineering technology of RA backfill subgrade by improving construction meth-

ods, optimizing test methods, and reinforcing quality control. This effort aims to enhance its bending fatigue performance and overall reliability.

(2) Improving the quality and stability of RA. The source and quality of RA directly influence its bending fatigue performance and durability. Hence, future research could focus on enhancing the preparation technology of RA, optimizing the selection and treatment methods of raw materials for aggregate, improving the quality and stability of RA, and enhancing its potential application in backfill subgrade.

(3) Strengthening the monitoring and evaluation of RA backfill subgrade. With the widespread application of RA backfill subgrade technology, it becomes crucial to monitor and evaluate its long-term service performance. Therefore, future research could enhance the monitoring and evaluation of deformation, crack propagation, and displacement of RA backfill subgrade under dynamic load conditions. This approach would provide a scientific basis for project management and maintenance.

Abbreviations

RA	Recycled aggregate

Symbols

A, A′	Variables related to fatigue damage accumulation
DF	Fatigue damage variable
maxH	Upper limit of effective stress
α, β	Stress and displacement variables
dα, dβ	Derivatives of stress and displacement variables
V	Creep damage of RA
J	Fatigue damage of RA
FRT	Fatigue life equation
NF	Fatigue damage model equation
δ0	Initial strain of the edge
ε1	Effective tensile strain
Si, Qi, Ki	Structural parameters for RA subgrade
XC	Reduction factor of the equivalent stress model
B	Bending moment bearing capacity

Greek symbols

ψ1, ψ0	Elastic modulus after and before fatigue damage

Subscripts

i	Denotes indices in formulae

Superscripts

-	Denotes reference or ideal values

Acknowledgements
Not applicable

Authors' contributions
Chen Zehui: writing—original draft preparation, conceptualization, supervision, project administration. Feng Xiaowei: methodology, software. Fang Xinjun: formal analysis, validation. Wu Shijun: language review.

Funding
This work is supported by Zhejiang Provincial Department of Education Research Project Funding (Y202352606).

Availability of data and materials
The raw data supporting the conclusions of this article will be made available by the authors, without undue reservation.

Declarations

Competing interests
The authors declare that they have no competing interests.

Received: 27 April 2024 Accepted: 7 July 2024
Published online: 22 July 2024

References

1. Agarwal A, Ramana GV, Datta M, Soni NK, Satyakam R (2023) Pullout behaviour of polymeric strips embedded in mixed recycled aggregate (MRA) from construction & demolition (C&D) waste–effect of type of fill and compaction. Geotext Geomembranes 51:405–17
2. Zhang X, Liu X, Zhang S, Wang J, Fu L, Yang J, Huang Y (2023) Analysis on displacement-based seismic design method of recycled aggregate concrete-filled square steel tube frame structures. Struct Concr 24:3461–3475
3. Zhang J, Liu X, Liu J, Zhang M, Cao W (2023) Seismic performance and reparability assessment of recycled aggregate concrete columns with ultra-high-strength steel bars. Eng Struct 277:115426
4. Shi W, Liu Y, Wang W, Duan P, Wang Z, Shang Z (2023) Relationship between chloride ion permeation resistance of recycled aggregate thermal insulation concrete and pore structure parameters. Constr Build Mater 370:130666
5. Dong JF, Guan ZW, Chai HK, Wang QY (2023) High temperature behaviour of basalt fibre-steel tube reinforced concrete columns with recycled aggregates under monotonous and fatigue loading. Constr Build Mater 389:131737
6. Shang X, Chen Y, Qi Y, Chang J, Yang J, Qu N (2023) Comparative life cycle environmental assessment of recycled aggregates concrete blocks using accelerated carbonation curing and traditional methods. Constr Build Mater 404:133207
7. Huang J, Li W, Ma Y, Jin M, Li Z, Manzano H, Liu J (2023) Multiscale deterioration of recycled aggregate gel network via solar irradiation: reaction molecular dynamics and experiments. J Clean Prod 426:139084
8. Wang J, Ma G, Yang W (2020) Finite element simulation of recycled large aggregate self-compacting concrete short columns with steel tubes. IOP Conference Series: Earth and Environmental Science, vol 525. IOP Publishing, p 012178
9. Mo KH, Ling TC, Cheng Q (2021) Examining the influence of recycled concrete aggregate on the hardened properties of self-compacting concrete. Waste Biomass Valorization 12:1133–1141
10. Fiol F, Revilla-Cuesta V, Skaf M, Thomas C, Manso JM (2023) Scaled concrete beams containing maximum levels of coarse recycled aggregate: structural verifications for precast-concrete building applications. Struct Concr 24:3476–3497
11. Fayed S, Madenci E, Özkiliç YO, Mansour W (2023) Improving bond performance of ribbed steel bars embedded in recycled aggregate concrete using steel mesh fabric confinement. Constr Build Mater 369:130452
12. Luo B, Wang D, Mohamed E (2023) The process of optimizing the interfacial transition zone in ultra-high performance recycled aggregate concrete through immersion in a water glass solution. Mater Lett 338:134056
13. Huang L, Xie J, Huang J, Li L, Lu Z, Huang P (2023) Compressive behaviour of GFRP-confined geopolymeric recycled aggregate concrete: effects of RA content, GRAC size and confinement ratio. Eng Struct 291:116421
14 Zhao HY, Han LH, Hou C, Lyu WQ (2023) Performance of recycled aggregate concrete-filled high-strength steel tubes under axial compression, tension and torsion. Thin-Walled Struct 184:110478
15. Tung TM, Babalola OE, Le D-H (2023) Evaluation of the post fire mechanical strength properties of recycled aggregate concrete containing GGBS: optimization and prediction using machine learning techniques. Asian J Civ Eng 24:1639–1666
16. Chen Y, He Q, Liang X, Chen Z, Li H (2023) Experimental investigation on mechanical properties of steel fiber reinforced recycled aggregate concrete under uniaxial cyclic compression. Constr Build Mater 387:131616
17 Kazemi R (2023) Artificial intelligence techniques in advanced concrete technology: a comprehensive survey on 10 years research trend. Eng Rep 5:e12676
18. Liu G, Tošić N, de la Fuente A (2023) Recycling of macro-synthetic fiber-reinforced concrete and properties of new concretes with recycled aggregate and recovered fibers. Appl Sci 13:2029
19. Fan Z, Liu H, Liu G, Wang X, Cui W (2023) Compressive performance of fiber reinforced recycled aggregate concrete by basalt fiber reinforced polymer-polyvinyl chloride composite Jackets. J Renew Mater 11:1763–1791
20. Adessina A, Ben Fraj A, Barthélémy JF (2023) Improvement of the compressive strength of recycled aggregate concretes and relative effects on durability properties. Constr Build Mater 384:131447
21. Revilla-Cuesta V, Skaf M, Chica JA, Ortega-López V, Manso JM (2023) Quantification and characterization of the microstructural damage of recycled aggregate self-compacting concrete under cyclic temperature changes. Mater Lett 333:133628
22. Ghosn S, Hamad B, Awwad E (2023) Structural and life cycle assessments of recycled aggregate concrete beams incorporating industrial hemp fibers. Struct Concr 24:7742–7758
23. Cui H, Xing C, Cheng W, Yang X and Wang W (2020) Influencing factors and significant analysis of mechanical properties of silty clay subgrade in seasonal frozen area. Advances in Environmental Vibration and Transportation Geodynamics: Proceedings of ISEV 2018. Springer, pp 179–92
24. Kanagaraj B, Kiran T, N A, Aljabri K, S J (2023) Development and strength assessment of eco-friendly geopolymer concrete made with natural and recycled aggregates. Constr Innov 23:524–45
25. Simões YS, Fernandes FPD, Castro AL, Munaiar Neto J (2023) Experimental and numerical analysis of the thermal and mechanical behaviour of steel and recycled aggregate concrete composite elements exposed to fire. Fire Mater 47:139–155
26. Tuladhar R, Marshall A and Sivakugan N (2020) Use of recycled concrete aggregate for pavement construction. Advances in construction and demolition waste recycling. Elsevier, pp 181–97

Publisher's Note